Multifunctional Ternary Semitransparent Organic Solar Cell Module with area above 100 cm^2 and Average Visible Transmittance above 30%

Juxuan Xie,[a] Ju Zhao,[a] Zhisheng Zhou,[a] Kai Zhang,*[a] Jiangkai Yu,[a] Chang Zhu,[a] and Fei Huang*[a]

[a] Institute of Polymer Optoelectronic Materials and Devices, State Key Laboratory of Luminescent Materials and Devices, South China University of Technology, Guangdong Basic Research Center of Excellence for Energy & Information Polymer Materials, Guangzhou 510640, P. R. ChinaE-mail: Correspondence should be addressed to e-mail: mszhangk@scut.edu.cn; msfhuang@scut.edu.cn

Experimental Section

1. Materials

Glass/ITO substrates with 100 cm² modules were purchased from Advanced Election Technology Co., Ltd, while those with 21 cm² modules were obtained from South China Science & Technology Company Limited. PTzBI-Cl, DT-Y6, and PNDIT-F3N were purchased from Dongguan VOLT-AMP Optoelectronic Technology Co., Ltd. BTR-Cl was purchased from Solarmer Materials Inc. The PEDOT:PSS (CLEVIOS P VP Al4083) was purchased from Heraeus Clevios. All materials and solvents were commercially available.

2. Small-area Devices Fabrication

The Opaque OSCs were fabricated according to the device structure of ITO/PEDOT:PSS/BHJ/PNDIT-F3N/Ag (100 nm). Firstly, the patterned ITO substrates were subsequently cleaned with deionized water and isopropanol for 30 min, then dried in a vacuum oven at 60 °C for 12 h. Secondly, PEDOT:PSS was spin-coated onto the plasma-treated ITO substrates at 3500 rpm for 30 s and annealed at 150 °C for 15 min. The active layer solution was prepared by using the PTzBI-Cl:DT-Y6 or the PTzBI-Cl:BTR-Cl:DT-Y6 solute and toluene solvents at a concentration of 10 mg/mL. The active layer solution was spin-coated on PEDOT:PSS films, followed by annealing at 100 °C for 10 min. Then, the PNDIT-F3N solution was spin-coated at 2000 rpm for 30 s onto the active layer. Finally, the 100 nm Ag layer was evaporated in a high vacuum chamber of 3×10^{-6} Pa. The Semitransparent OSCs were fabricated according to the device structure of ITO/PEDOT:PSS/BHJ/PNDIT-F3N/Ag (10 nm, 15 nm, 20 nm, and 30 nm)/MoO_3.

3. Large-area modules fabrication

The 21 cm² module consists of seven interconnected sub-cells, while the 100 cm² module consists of thirteen interconnected sub-cells. For Opaque modules, active layer solution (PTzBI:BTR-Cl:DT-Y6=1:0.2:1.2, in toluene) deposited on PEDOT:PSS films by blade-coating with a coating velocity of 6 mm/s and gap height of 200 μm, followed by annealing at 90 °C for 10 min in N_2 protected glove box. The semi-transparent module was fabricated using the same device process to the opaque module. Finally, the 100 nm Ag layer (15 nm Ag for semitransparent modules) was evaporated in a high vacuum chamber of 3×10^{-6} Pa.

4. Characterization

Keithley 2400 was used to measure the current density (J)-voltage (V) characteristics of small-area devices. The photovoltaic parameters of small-area devices were obtained under 1sun AM1.5G spectra by using a class solar simulator test system (Enlitech Technology Company). The light intensity (100 mW cm^{-2}) was calibrated by China General Certification Center (CGC) certified reference monocrystal silicon cell (Enlitech). The photovoltaic parameters of small-area devices were obtained under 1sun AM1.5G spectra by using an Enli Solar simulator, and the beam size is 12 cm×12 cm. QE-R test system (Enlitech) was used to measure the EQE date. UV-vis absorption spectra and transmittance were measured by the ultraviolet-visible spectrophotometer (SHIMADZU UV-3600). Before each test, the light intensity (100 mW cm^{-2}) was calibrated as a reference monocrystal silicon cell (Enlitech). The surface morphologies of the OSCs films were characterized using an atomic force microscope (NanoMan) and a transmission electron microscope (JET-2100F). Grazing incidence wide-angle X-ray scattering (GIWAXS) measurements were conducted using a Xeuss 2.0.

SCLC Measurements: Electron and hole mobility were calculated from the space-charge-limited current (SCLC) method. The hole-only device structures were ITO/PEDOT:PSS/BHJ/MoO_3/Ag. The electron-only device structures were ITO/ZnO/BHJ/PNDIT-F3N/Ag. The mobility was calculated by fitting the dark current to the model of a single-carrier SCLC, which is described by the equation: $J = (9/8)\varepsilon_o\varepsilon_r\mu((V_2)/(d_3))$. Where J is current density, μ is the zero-field mobility, ε_o is the permittivity of the free space, ε_r is the relative permittivity of the material, d is the thickness of the active layers, and V is the effective voltage.

Optical simulation: Under the premises that the layers are homogeneous, and their optical response can be characterized by a complex refractive index (N=n+k×i), the transfer matrix method (TMM) was utilized to forecast the reflection and transmission at each interface, as well as the interference throughout the entire device. Optical simulation of the Glass/ITO/PEDOT:PSS/BHJ/PNDIT-F3N/Ag stack was performed to investigate the normalized optical electric field intensity $|E|^2$. Five steps were involved in conducting the optical simulation using MATLAB. Firstly, the refractive index (η) and extinction coefficient (k) were measured using an ellipsometer (ME-L ellipsometer, Wuhan Eoptics Technology Co., Wuhan, China). Secondly, Set up the optical function: $Y_1,Y_2,\cdots,Y_j,\cdots Y_n = F(\tilde{n}_1,\tilde{n}_2,\cdots,\tilde{n}_j,\cdots,\tilde{n}_m,d_1,d_2,\cdots,d_j,\cdots,d_m)$, where Y_1 is the ith characteristic of the device, $\tilde{n}_j = \eta_j + i \times \kappa_j$ is the complex refractive index of the j_{th} film, and d_j is the thickness of the j_{th} film. Finally, the photoelectric field $|E|^2$ in the devices should be calculated using TMM.

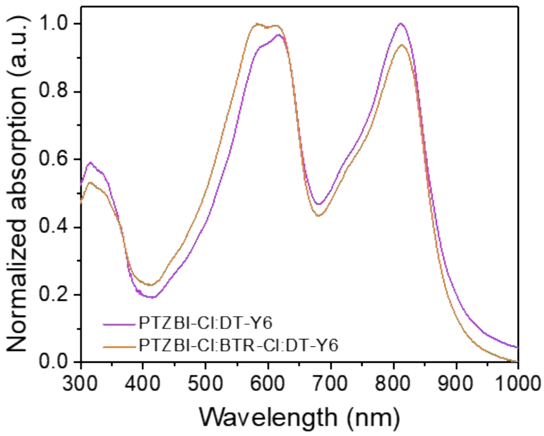

Figure S1. The absorption of PTzBI-Cl:DT-Y6 and PTzBI-Cl:BTR-Cl:DT-Y6 films.

Ratio	V_{oc} (V)	J_{sc} (mA cm^{-2})	FF (%)	PCE$_{avg}$ (%)	PCE$_{max}$ (%)	AVT$_{pure}$ (%) [a)]
0	0.860±0.002	25.2±0.2	74.6±0.4	16.2±0.0	16.2	50.9
5%	0.850±0.001	25.5±0.1	76.7±0.3	16.6±0.0	16.6	50.5
10%	0.851±0.003	25.9±0.1	77.2±0.3	17.0±0.0	17.0	49.8
15%	0.853±0.004	24.4±0.1	77.5±0.7	16.1±0.1	16.2	46.1

Table S1. Photovoltaic parameters of devices at different BTR-Cl weight ratios.

a) The average transmittance of the pure active layer films in the visible light region.

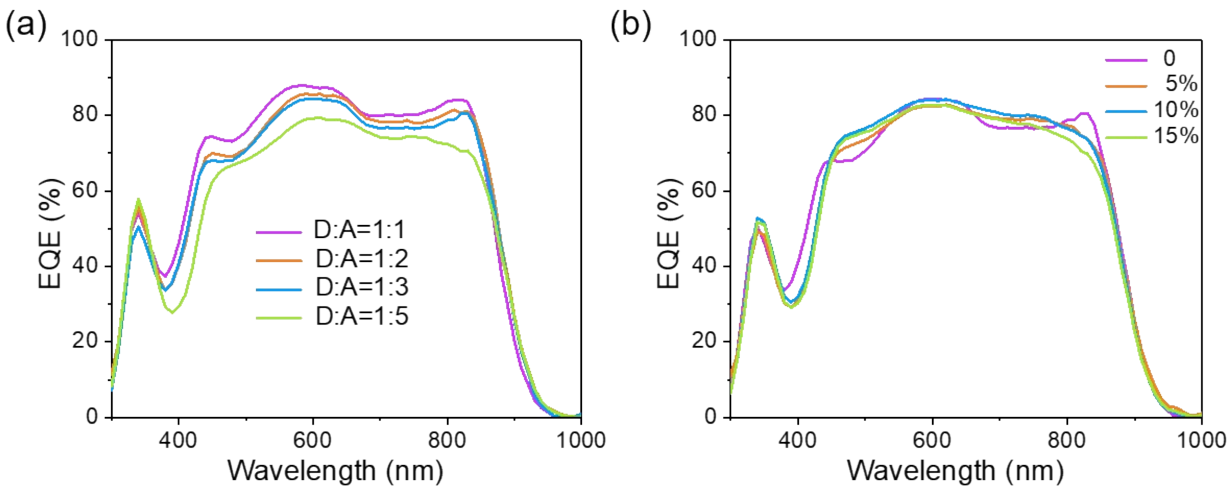

Figure S2. (a) EQE spectra of different D/A weight ratios. (b) EQE spectra of different BTR-Cl ratios.

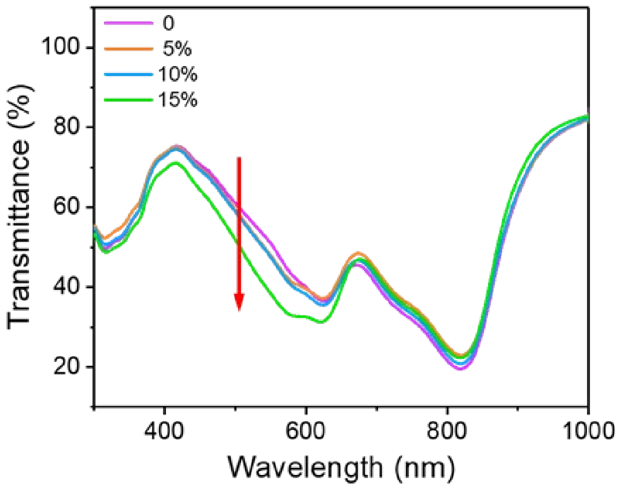

Figure S3. Transmittance spectra of films with different BTR-Cl ratios.

Table S2. The relevant parameters of the J_{ph}-V_{eff} curves.

	V_0(V)	J_{ph}(mA/cm2)	J_{sat}(mA/cm2)	G_{max}(m^{-3}/s)	P(E,T) (%)	L(nm)
w/o	0.85	25.08	25.56	1.59×10^{27}	98.12	110
w BTR-Cl	0.86	26.16	26.59	1.62×10^{27}	98.38	110

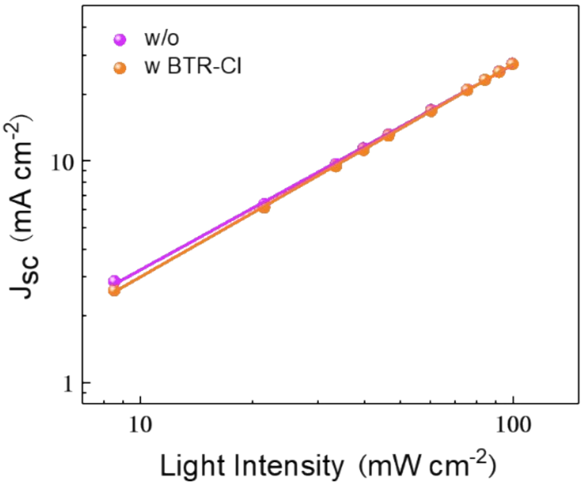

Figure S4. Light intensity dependence of J_{sc} of devices with and without BTR-Cl additive.

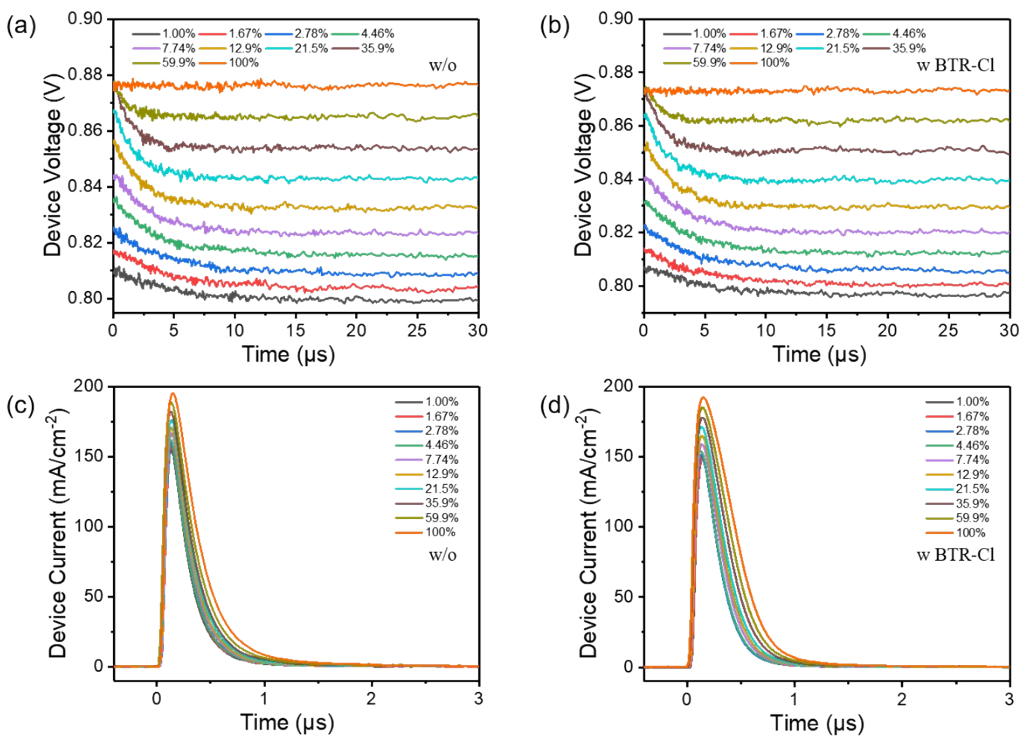

Figure S5. Transient photovoltage and charge extraction measurements. Transient photovoltage (a,b) and charge extraction (c,d) traces under different illumination intensities.

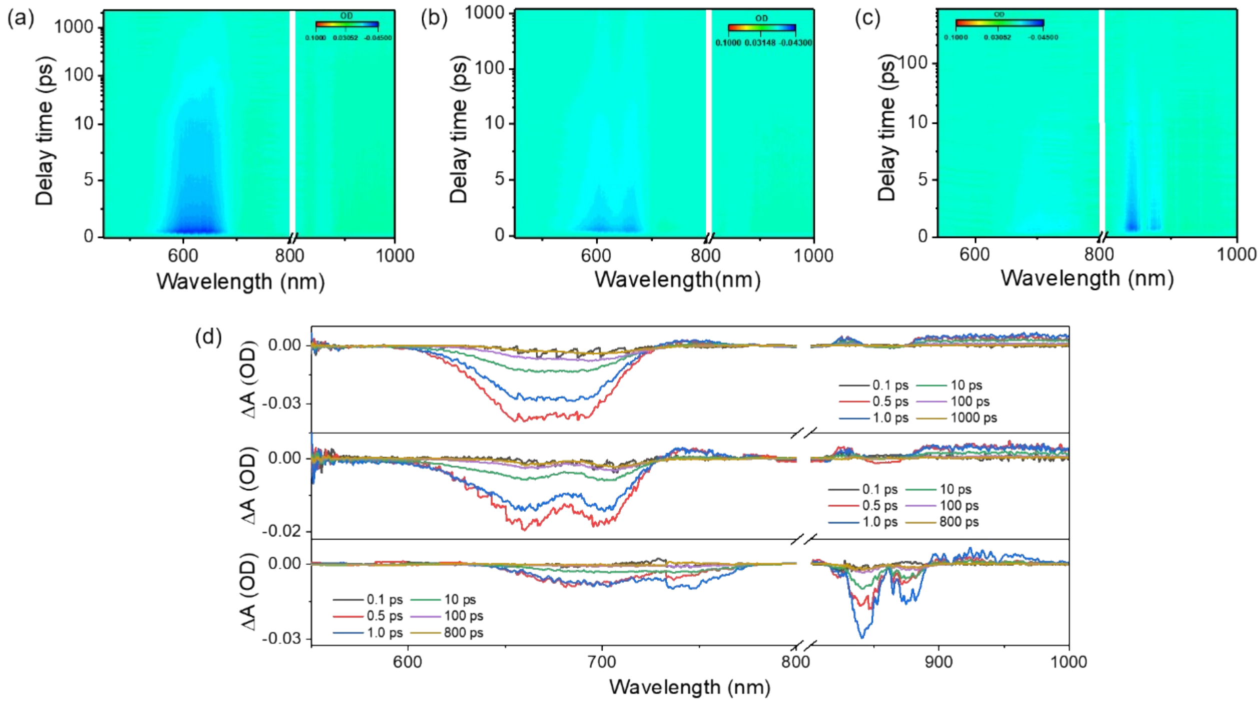

Figure S6. 2D color plots of TA spectra of a) PTzBI-Cl, b) BTR-Cl and c) DT-Y6 neat films. d) TA spectra of PTzBI-Cl, BTR-Cl, and DT-Y6 neat films.

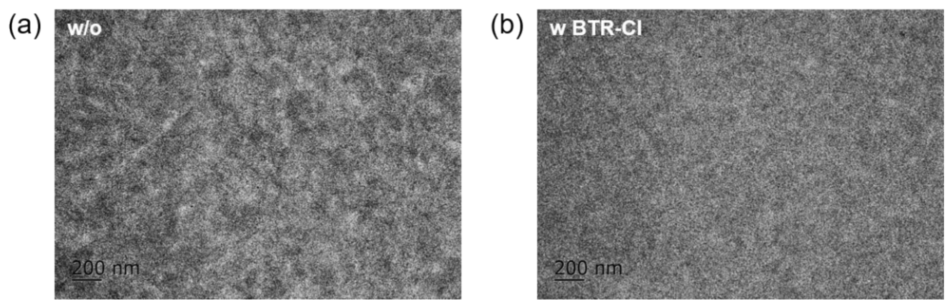

Figure S7. TEM image of (a) PTzBI-Cl:DT-Y6 blend film, (b) PTzBI-Cl:BTR-Cl:DT-Y6 blend film.

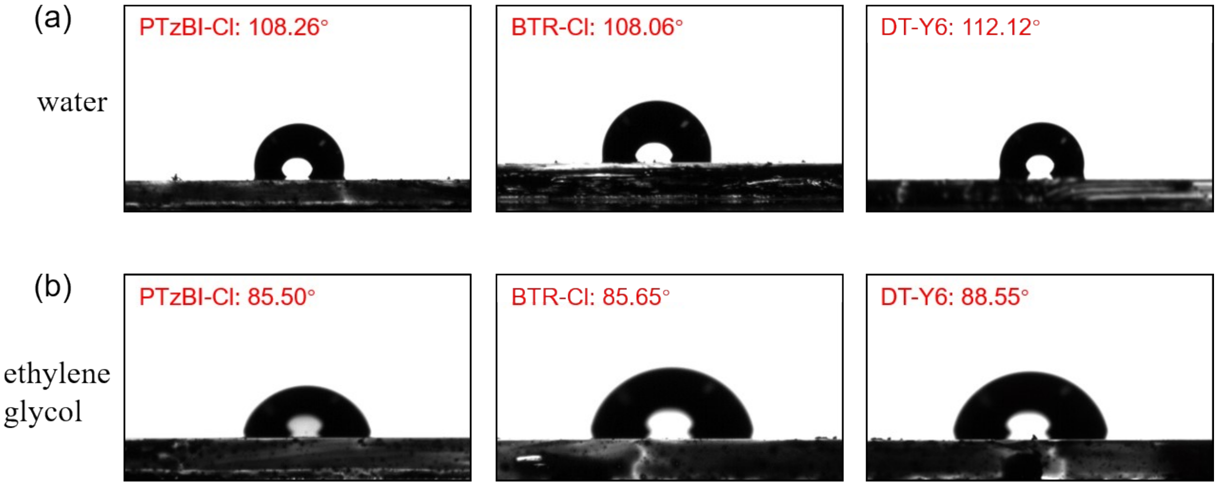

Figure S8. Contact angles of (a) water and (b) ethylene glycol on neat PTzBI-Cl, BTR-Cl, and DT-Y6 films.

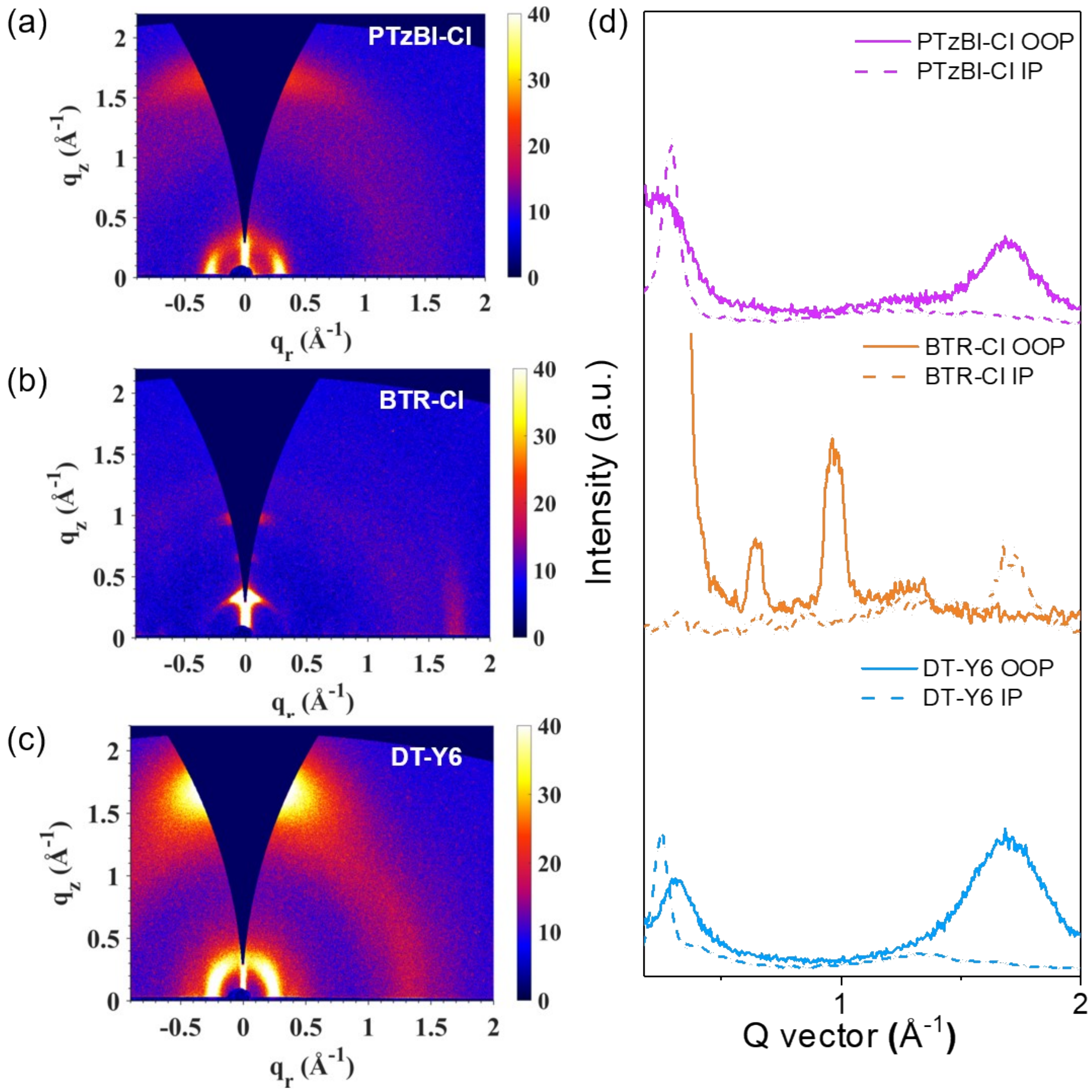

Figure S9 2D GIWAXS pattern of (a) PTzBI-Cl neat film, (b) BTR-Cl neat film, and (c) DT-Y6 neat film. (d) 1D profiles of out-of-plane direction and in-plane direction of PTzBI-Cl, BTR-Cl, and DT-Y6 neat films.

Table S3 Molecular packing parameters of corresponding films.

Sample	Peak	Peak location ($Å^{-1}$)	π-π stacking distance (Å)	FWHM ($Å^{-1}$)	Crystal coherence length (Å)
PTzBI-Cl	(100) In IP	0.280	/	0.070	80.02
	(010) In OOP	1.693	3.727	0.182	30.95
BTR-Cl	(010) In IP	1.720	3.665	0.153	36.91
DT-Y6	(100) In IP	0.251	/	0.060	90.00
	(010) In OOP	1.703	3.719	0.335	16.85
PTzBI-Cl: DT-Y6	(100) In IP	0.285	/	0.075	74.52
	(010) In OOP	1.721	3.710	0.306	18.46
PTzBI-Cl:BTR-Cl:DT-Y6	(100) In IP	0.290	/	0.079	70.84
	(010) In OOP	1.729	3.690	0.280	20.15

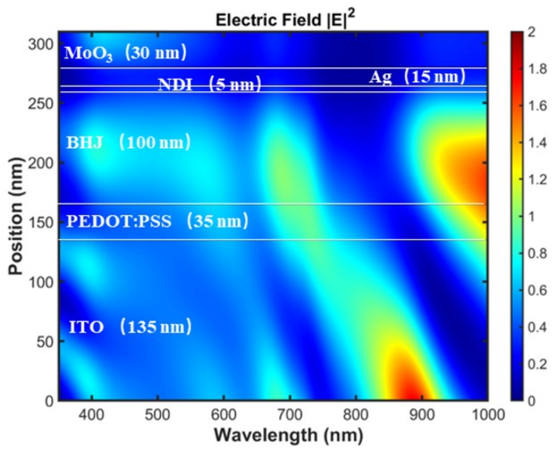

Figure 10. Simulated electric field intensity $|E|^2$ of ST-OSC with MoO_3.

Table S4. Photovoltaic performance parameters and optical parameters of different Ag thicknesses.

Thickness (nm)	V_{oc} (V)	J_{sc} (mA cm^{-2})	FF (%)	PCE$_{avg}$ (%)	PCE$_{max}$ (%)	AVT (%)	LUE (%)	CRI	CIE
10	0.848±0.001	19.8±0.1	72.6±0.9	12.2±0.1	12.3	29.3	3.5	87	(0.2606,0.2790)
15	0.851±0.002	21.1±0.2	74.3±0.8	13.3±0.2	13.5	28.5	3.8	84	(0.2553,0.2808)
20	0.851±0.001	22.0±0.1	76.1±0.5	14.3±0.0	14.3	25.1	3.5	79	(0.2252,0.2394)
30	0.852±0.003	24.5±0.2	76.7±0.6	15.8±0.1	15.9	15.1	2.4	73	(0.2116,0.2024)

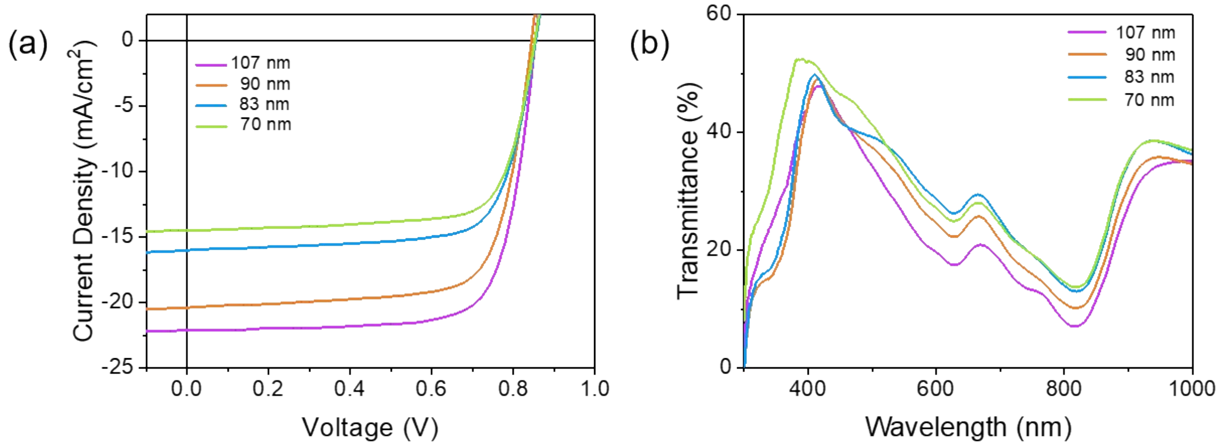

Figure S11. (a) J-V curves of BHJ with different film thicknesses, (b) The transmittance spectra of BHJ with different film thicknesses.

Table S5. Photovoltaic performance parameters and optical parameters of different film thicknesses.

Thickness (nm)	V_{oc} (V)	J_{sc} (mA cm^{-2})	FF (%)	PCE_{avg} (%)	PCE_{max} (%)	AVT (%)	LUE (%)	CRI	CIE
107	0.851±0.002	21.1±0.3	74.3±0.8	13.3±0.2	13.5	28.5	3.8	84	(0.2553,0.2808)
90	0.851±0.002	19.5±0.1	75.0±0.2	12.5±0.1	12.6	31.4	3.9	82	(0.2704,0.3093)
83	0.851±0.003	15.6±0.4	73.9±0.9	9.8±0.1	9.9	34.1	3.4	83	(0.2708,0.3093)
70	0.849±0.003	14.5±0.0	73.6±0.3	9.1±0.0	9.1	35.0	3.2	84	(0.2823,0.3227)

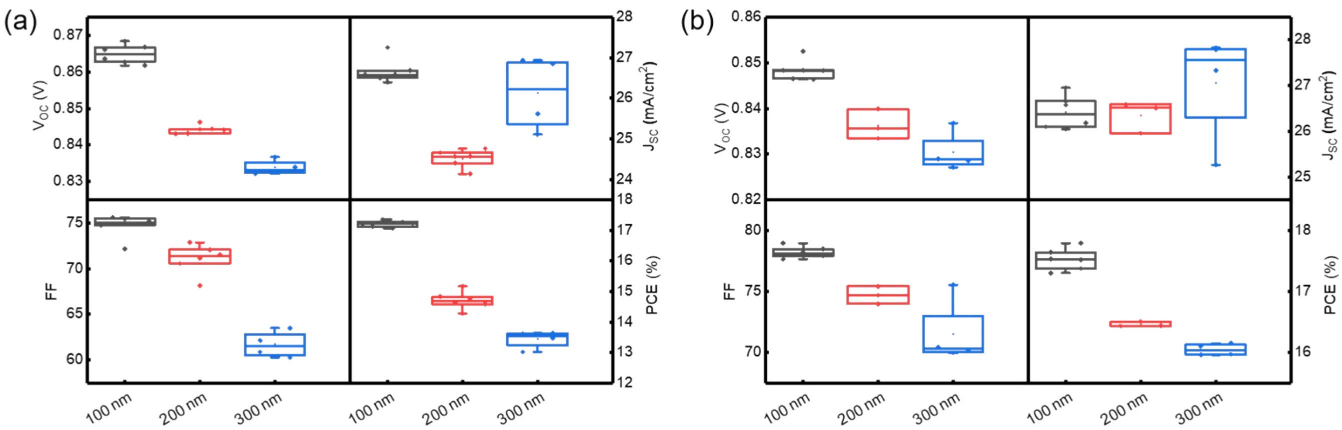

Figure S12. Photovoltaic performance box diagrams of (a) PTzBI-Cl:DT-Y6 and (b) PTzBI-Cl:BTR-Cl:DT-Y6 at thicknesses of 100, 200 and 300 nm, respectively.

Table S6. Photovoltaic parameters of PTzBI-Cl:DT-Y6 and PTzBI-Cl:BTR-Cl:DT-Y6 at thicknesses of 100, 200 and 300 nm, respectively.

	Thickness (nm)	V_{oc} (V)	J_{sc} (mA cm^{-2})	FF (%)	PCE_{avg} (%)	PCE_{max} (%)
PTzBI-Cl:DT-Y6	100	0.865±0.003	26.6±0.3	74.7±1.2	17.2±0.1	17.3
	200	0.844±0.001	24.5±0.2	71.1±1.6	14.7±0.3	15.0
	300	0.834±0.002	26.1±0.9	61.7±1.4	13.4±0.2	13.6
PTzBI-Cl:BTR-Cl:DT-Y6	100	0.848±0.002	26.4±0.3	78.2±0.4	17.5±0.2	17.7
	200	0.836±0.003	26.4±0.3	74.6±0.7	16.5±0.0	16.5
	300	0.830±0.004	27.0±1.2	71.5±2.6	16.0±0.1	16.1

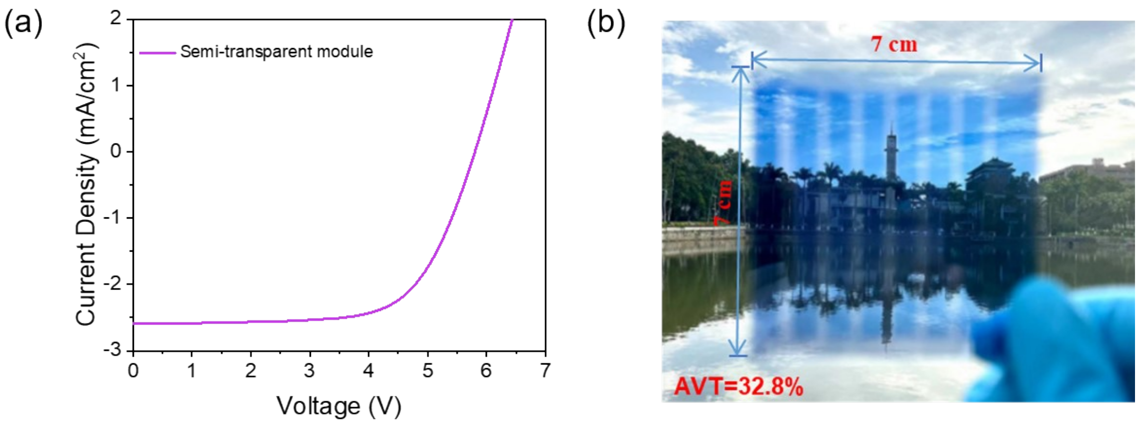

Figure S13. (a) *J–V* curve of semi-transparent module based on PTzBI-Cl:BTR-Cl:DTY6. (b) The photograph of a semitransparent module for demonstration.

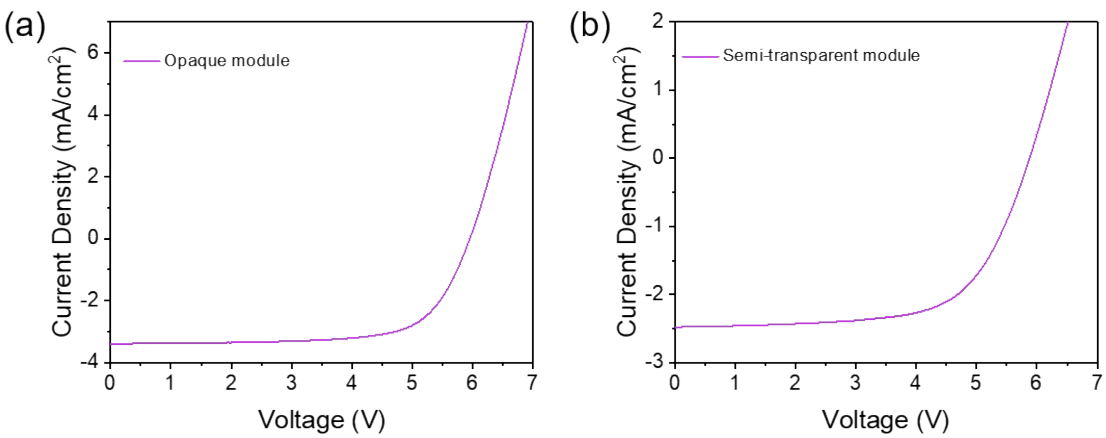

Figure S14. (a) *J–V* curve of Opaque module based on PTzBI-Cl:DTY6. (b) *J–V* curve of semi-transparent module based on PTzBI-Cl: DTY6.

Table S7. Photovoltaic performances of large-area modules (21 cm^2) based on PTzBI-Cl:DTY6 under illumination of AM 1.5G, 100 mW cm^{-2}.

Device Type	V_{oc} (V)	J_{sc} (mA cm^{-2})	FF (%)	PCE_{avg} (%)	PCE_{max} (%)	AVT (%)	LUE (%)	IRR （%）	CRI	CIE
Opaque	5.8±0.1	3.3±0.1	70.2±0.3	14.0±0.1	14.1					
ST	5.8±0.1	2.4±0.1	64.7±0.3	9.4±0.0	9.4	32.8	3.0	75.2	83.9	(0.267,0.297)

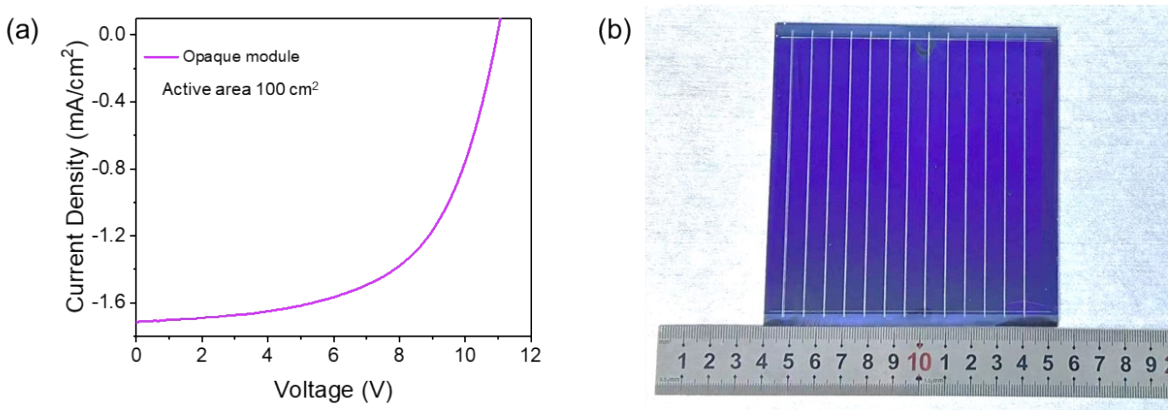

Figure S15. (a) *J-V* curve of opaque module (active area 100 cm^2) based on PTzBI-Cl:BTR-Cl:DTY6, (b) The photograph of an opaque OSC module.

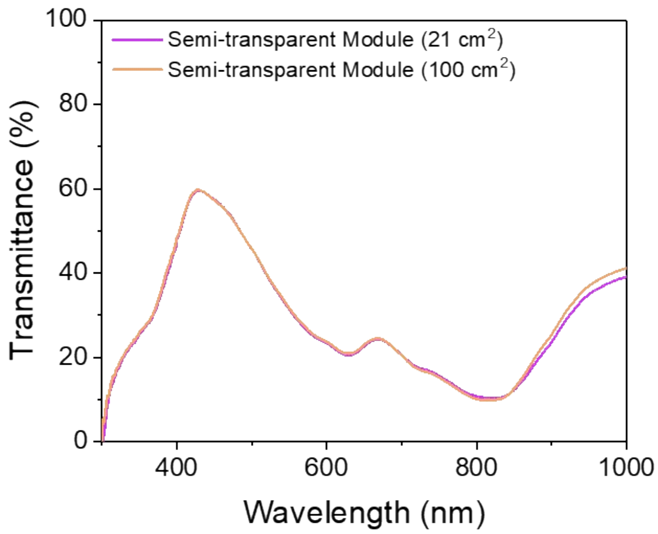

Figure S16. The transmittance spectra of the semitransparent module.

Table S8. The summary of PCEs obtained from recently reported large-area organic photovoltaic devices with active areas over 10 cm^2.

Active layer	Coating method	Active area (cm^2)	PCE (%)	Ref.
PM6:Y6:$PC_{61}BM$	blade coating	26.2	12.6	[1]
PBDB-T:ITIC	slot-die coating	15	8.9	[1]
PTB7-Th:COi_8DFIC:$PC_{71}BM$	slot-die coating	25	$10.1^{a)}$	[1]
PTB7-Th:COi_8DFIC:$PC_{71}BM$	slot-die coating	50	$9.05^{a)}$	[1]
PM6:Y6:$PC_{71}BM$	spin coating	10.1	12.6	[1]
PM6:Y6:$PC_{71}BM$	spin coating	54	13.2	[1]
PM6:DTY6	blade coating	18	$14.4^{a)}$	[1]
SMD2:ITIC-Th	slot-die coating	80	5.25	[1]
P3HT:*o*-IDTBR	blade coating	59.5	4.7	[1]
TPD-3F:IT-4F	blade coating	20.4	$10.4^{a)}$	[2]
PM6:Y6	blade coating	36	7.31	[2]
PM6:Y6:BTO:PC71BM	blade coating	36	14.26	[2]

PNTz4T-5MTC:PCBM	bar coating	54.45	6.61[a)]	[2]
PTB7-Th:T2-OEHRH	bar coating	55.5	9.32[a)]	[2]
PBDB-T:CNDTBTC8IDT-	bar coating	54.45	9.21	[2]
PBDB-TF:IT-4F	blade coating	58.5	9.03	[2]
PBDB-T-2F:N3:P(NDI2OD-T2)	blade coating	20.61	14.31	[2]
PBDB-T-2F:N3:P(NDI2OD-T2)	blade coating	58.5	14.04	[2]
PM6/Y6	blade coating	36	13.47	[3]
PB2:FTCC-Br:BTP-eC9	blade coating	10	15.9	[4]
PB2:FTCC-Br:BTP-eC9	blade coating	15	15.3	[4]
PB2:FTCC-Br:BTP-eC9	blade coating	20	14.5	[4]
PB2:FTCC-Br:BTP-eC9	blade coating	50	15.2	[4]
PBQx-TF:eC9-2Cl	blade coating	20	15.1[a)]	[5]
PM6:Qx-1	slot-die coating	15	12.3[a)]	[6]
PM6:CH7	blade coating	25.2	14.42[a)]	[7]
PM6:Y7-BO:PC71BM:BTA-Erh	D-bar coating	55	12.2	[8]
PM6: BO-4Cl:m-BTP-PhC6	spin coating	19.3	16.04	[9]
PM6:BTP-eC9	meniscus-guided coating	25	11.29[a)]	[10]
PM6:BTP-BO-4Cl	blade coating	18.73	14.79[a)]	[11]
PM6:BTP-eC9:L8-BO: BTP-S10	blade coating	67.915	12.2	[12]
PM6:Y6:ITIC:PC71BM	spin coating	19.34	13.25	[13]
TPD-3:Y6	spin coating	20.4	9.31	[14]
D18:DTC11	blade coating	21	15.4[a)]	[15]
PM6:BTP-eC9/IO-4Cl	spin coating	15.48	13.24	[16]
PM6:L8-BO	blade coating	18.73	15.2[a)]	[17]
PM6-PBDBT(55):IPC1CN-BBO-IC2Cl	blade coating	58.5	11.28[a)]	[18]
PBDB-T-2F:L8-BO	blade coating	10.8	9.54	[19]
PM6:L8-BO:PJ1	slot-die coating	30	13.08[a)]	[20]
PM6:P2:L8-BO	bar coating	55	13.88[a)]	[21]

PM6:PBQx-TCl:PY-IT	spin coating	19.3	16.26[a)]	[22]
PTVT-T:GS60	blade coating	22	11.2[a)]	[23]
PTQ10:BTP-4F-12:PC71BM	blade coating	10.17	10.77[a)]	[24]
PM6:Y6-C12:PC61BM	blade coating	204	15.0[a)]	[25]
PBQx-TF:eC9-2Cl	slot-die coating	21.9	15.8[a)]	[26]
D18:L8-BO	spin coating	19.8	15.44	[27]
D18:L8-BO:PY-TPT	blade coating	16.6	13.84[a)]	[28]
PM6:L8-BO:BTO-BO	spin coating	15.03	16.35[a)]	[29]
PM6:D18:L8-BO	blade coating	15.6	16.03[a)]	[30]
PM6:D18:L8-BO	blade coating	72	14.45[a)]	[30]
PM6:BTP-ec9	blade coating	28.82	16.04[a)]	[31]
PM6:BTP-ec9	blade coating	16.94	14.58[a)]	[32]
PM6:BO-4Cl	spin coating	19.31	15.74[a)]	[33]
D18-N-m-10:L8-BO	slot-die coating	43	12.43	[34]
PTzBI-Cl:BTR-Cl:DT-Y6	blade coating	21	15.2[a)]	This work
PTzBI-Cl:BTR-Cl:DT-Y6	blade coating	100	11.04	This work

a) The related large-area devices were fabricated by non-halogen solvents.

Table S9. The summary of PCEs obtained from recently reported large-area semi-transparent organic photovoltaic devices with active areas over 10 cm^2.

Active layer	Coating method	Active area (cm^2)	PCE (%)	AVT (%)	Ref.
P3HT:PCBM	spray coating	30	1.8	30	[35]
PBTZT-stat-BDTT-8:PV-A600	slot-die coating	114.5	4.5	20	[36]
PBDTTT-EFT:PC71BM	blade coating	216	4.5	10	[37]
PBDTTT-EFT:PC71BM	blade coating	216	4.97	8.25	[37]
P3HT:IDTBR	blade coating	60	5	6.2	[38]
PBDB-T:ITIC:PC71BM	blade coating	216	7.7	8.25	[39]
PM6:DTY6	blade coating	18	11.6	10.8	[40]
PM6:DTY6	blade coating	18	9.8	14.5	[40]
PM6:DTY6	blade coating	18	7.1	18.7	[40]
PTB7:PC70BM	spin coating	18.63	8.22	41.25	[41]
PCE-10:BT-CIC:TT-FIC	spin coating	12.8	7.5	3.2	[42]
PM6:Y6-hu	bar coating	36.22	10.47 (red)	-	[43]
PM6:Y6-hu	bar coating	36.22	10.01(greed)	-	[43]
PM6:Y6-hu	bar coating	36.22	10.39 (blue)	10.05	[43]
J52-Cl:BTA3:BTA1	spin coating	12	5.88	20.8	[44]
PM6:BTP-BO-4Cl	blade coating	18.73	12.01	22.3	[11]
PM6:BO-4Cl:m-BTP-PhC6	spin coating	18.61	11.28	-	[11]
PVX	slot-die coating	22.5	6.20	17.01	[45]
PVX	slot-die coating	45	7.8	17.01	[45]
PVX	slot-die coating	60	7.1	20.5	[46]
PVX	slot-die coating	60	5.9	28.3	[46]
PVX	slot-die coating	60	4.4	36.1	[46]
PTQ10:BTP-4F-12:PC71BM	blade coating	10.17	9.75	11.3	[24]

PTB7-Th:IEICO-4F	blade coating	56	3.5	56	[47]
PM6:Y6:PCBM	-	54	8.17	36.67	[48]
PTzBI-Cl:BTR-Cl:DT-Y6	blade coating	21	10.22	32.8	This work
PTzBI-Cl:BTR-Cl:DT-Y6	blade coating	100	6.71	32.9	This work

References

1. P. Xue, P. Cheng, R. P. S. Han, X. Zhan, *Mater. Horiz.*, 2022, **9**, 194-219.
2. S. Rasool, J. Yeop, H. W. Cho, W. Lee, J. W. Kim, D. Yuk, J. Y. Kim, *Mater. Futures*, 2023, **2**, 032102.
3. J. Jing, Y. Dou, S. Chen, K. Zhang, F. Huang, *eScience*, 2023, **3**, 100142.
4. J. Wang, P. Bi, Y. Wang, Z. Zheng, Z. Chen, J. Qiao, W. Wang, J. Li, C. An, S. Zhang, X. Hao, J. Hou, *CCS Chem.*, 2023, **1**, 218-229.
5. J. Wang, Y. Wang, P. Bi, Z. Chen, J. Qiao, J. Li, W. Wang, Z. Zheng, S. Zhang, X. Hao, J. Hou, *Adv. Mater.*, 2023, **35**, 2301583.
6. Y. Shen, H. Zhang, J. Zhang, C. Tian, Y. Shi, D. Qiu, Z. Zhang, K. Lu, Z. Wei, *Adv. Mater.*, 2023, **35**, 2209030.
7. S. Zhang, H. Chen, P. Wang, S. Li, Z. Li, Y. Huang, J. Liu, Z. Yao, C. Li, X. Wan, Y. Chen, *Sol. RRL*, 2023, **7**, 2300029.
8. T. Gokulnath, J. Kim, H. Kim, J. Park, D. Song, H.-Y. Park, R. Kumaresan, Y. Y. Kim, J. Yoon, S.-H. Jin, *ACS Appl. Mater. Interfaces*, 2023, **15**, 19307-19318.
9. D. Wang, Y. Li, G. Zhou, E. Gu, R. Xia, B. Yan, J. Yao, H. Zhu, X. Lu, H.-L. Yip, H. Chen, C.-Z. Li, *Energy Environ. Sci.*, 2022, **15**, 2629-2637.
10. H. Li, S. Liu, X. Wu, Q. Qi, H. Zhang, X. Meng, X. Hu, L. Ye, Y. Chen, *Energy Environ. Sci.*, 2022, **15**, 2130-2138.
11. J. Fan, Z. Liu, J. Rao, K. Yan, Z. Chen, Y. Ran, B. Yan, J. Yao, G. Lu, H. Zhu, C. Li, H. Chen, *Adv. Mater.*, 2022, **34**, 2110569.
12. L. Zhan, S. Yin, Y. Li, S. Li, T. Chen, R. Sun, J. Min, G. Zhou, H. Zhu, Y. Chen, J. Fang, C. Ma, X. Xia, X. Lu, H. Qiu, W. Fu, H. Chen, *Adv. Mater.*, 2022, **34**, 2206269.
13. Z. Jia, Z. Chen, X. Chen, J. Yao, B. Yan, R. Sheng, H. Zhu, Y. (Michael) Yang, *Photon. Res.*, 2021, **9**, 324-330.
14. J. Wu, C. Liao, Y. Chen, R. M. Jacobberger, W. Huang, D. Zheng, K. Tsai, W. Li, Z. Lu, Y. Huang, M. R. Wasielewski, Y. Chang, T. J. Marks, A. Facchetti, *Adv. Energy Mater.*, 2021, **11**, 2102648.
15. Z. Zhong, S. Chen, J. Zhao, J. Xie, K. Zhang, T. Jia, C. Zhu, J. Jing, Y. Liang, L. Hong, S. Zhu, D. Ma, F. Huang, *Adv. Energy Mater*., 2023, **13**, 2302273.
16. Y. Liu, C. Xie, X. Dong, Y. Wang, W. Wei, K. Feng, S. Xiong, Y. Jiang, Y. Zhou, *Sol. RRL*, 2023, **7**, 2300642.

17. J. Xiang, Z.-X. Liu, H. Chen, C.-Z. Li. *Adv. Mater.*, 2023, **35**, 2303729.
18. P. Gopikrishna, J. Rhee, S. Yoon, D. Um, H. Jin, Y. Jun, H. Choi, H. J. Son, B. Kim, *Adv. Funct. Mater.*, 2023, **33**, 2305541.
19. W. Zha, L.-M. Chen, S. Sun, X. Gao, Y. Han, T. Liu, Q. Luo, Y.-C. Chao, H.-W. Zan, H.-F. Meng, X. Zhu, C.-Q. Ma, *Sol. RRL*, 2023, **7**, 2300322.
20. C. Tian, J. Zhang, Y. Shen, H. Zhang, Z. Zhang, D. Qiu, L. Zhang, Z. Wei, *Sol. RRL*, 2023, **7**, 2300349.
21. T. Gokulnath, H. Kim, J. Lee, B. H. Cho, H.-Y. Park, J. Jee, Y. Y. Kim, K. Kranthiraja, J. Yoon, S.-H. Jin, *Adv. Energy Mater.*, 2023, **13**, 2302538.
22. T. Chen, X. Zheng, D. Wang, Y. Zhu, Y. Ouyang, J. Xue, M. Wang, S. Wang, W. Ma, C. Zhang, Z. Ma, S. Li, L. Zuo, H. Chen, *Adv. Mater.*, 2023, **36**, 2308061,
23. J. Wang, Y. Wang, J. Li, Y. Yu, B. Bi, j. Qiao, Z. Chen, C. Wang, W. Wang, J. Dai, X. Hao, S. Zhang, J. Hou, *Angew. Chem. Int. Ed.* 2023, **62**, 202314362.
24. J. Wachsmuth, A. Distler, C. Liu, T. Heumüller, Y. Liu, C. M. Aitchison, A. Hauser, M. Rossier, A. Robitaille, M.-A. Llobel, P.-O. Morin, A. Thepaut, C. Arrive, I. McCulloch, Y. Zhou, C. J. Brabec, H.-J. Egelhaaf, *Sol. RRL*, 2023, **7**, 2300602.
25. R. Basu, F. Gumpert, J. Lohbreier, P.-O. Morin, V. Vohra, Y. Liu, Y. Zhou, C. J. Brabec, H.-J. Egelhaaf, A. Distler, *Joule*, 2024, 8, 970-978.
26. Y. Yu, J. Wang, Y. Cui, Z. Chen, T. Zhang, Y. Xiao, W. Wang, J. Wang, X.-T. Hao, J. Hou, *J Am Chem Soc*, 2024, **146**, 8697-8705.
27. Y. Li, Z. Jia, P. Huang, T. Liu, D. Hu, Y. Li, H. Liu, X. Lu, S. Lu, X. Yin, Y. Yang, Adv. Energy Mater., 2024, **14**, 2304000.
28. Y. Wei, X. Zhou, Y. Cai, Y. Li, S. Wang, Z. Fu, R. Sun, N. Yu, C. Li, K. Huang, Z. Bi, X. Zhang, Y. Zhou, X. Hao, J. Min, Z. Tang, W. Ma, Y. Sun, H. Huang, *Adv. Mater*., 2024, **https://doi.org/10.1002/adma.202403294**, 2403294.
29. H. Chen, W. Sun, R. Zhang, Y. Huang, B. Zhang, G. Zeng, J. Ding, W. Chen, F. Gao, Y. Li, Y. Li, *Adv. Mater*., 2024, **https://doi.org/10.1002/adma.202402350**, 2402350.
30. B. Zhang, W. Chen, H. Chen, G. Zeng, R. Zhang, H. Li, Y. Wang, X. Gu, W. Sun, H. Gu, F. Gao, Y. Li, Y. Li, *Energy Environ. Sci*., 2024, **17**, 2935-2944.
31. Z. Liu, Y. Fu, J. Wu, X. Yi, M. Zhao, M. Huang, J. Liu, Z. Xie, *Adv. Funct. Mater*. 2024, **https://doi.org/10.1002/adfm.202401558**, 2401558.
32. H. Wang, S. Liu, H. Li, M. Li, X. Wu, S. Zhang, L. Ye, X. Hu, Y. Chen, *Adv. Mater.*, 2024, **36**, 2313098.
33. Z. Jia, J. Pan, X. Chen, Y. Li, T. Liu, H. Zhu, J. Yao, B. Yan, Y. Yang, *Energy Environ. Sci*., 2024., **17**, 3908–3916
34. D. Qiu, C. Tian, H. Zhang, J. Zhang, Z. Wei, K. Lu, *Adv. Mater.*,2024, **https://doi.org/10.1002/adma.202313251**, 2313251.
35. J. E. Lewis, E. Lafalce, P. Toglia, X. Jiang, *Sol. Energy Mater. Sol. Cell*s, 2011, **95**, 2816-2822.
36. S. Berny, N. Blouin, A. Distler, H. J. Egelhaaf, M. Krompiec, A. Lohr, O. R. Lozman, G. E. Morse, L. Nanson, A. Pron, T. Sauermann, N. Seidler, S. Tierney, P. Tiwana, M. Wagner, H. Wilson, *Adv. Sci*., 2016, **3**, 1500342.
37. P. T. Tsai, K. C. Lin, C. Y. Wu, C. H. Liao, M. C. Lin, Y. Q. Wong, H. F. Meng, C. Y. Chang, C. L. Wang, Y. F. Huang, S. F. Horng, H. W. Zan, Y. C. Chao, *ChemSusChem*, 2017, **10**, 2778-2787.
38. S. Strohm, F. Machui, S. Langner, P. Kubis, N. Gasparini, M. Salvador, I. McCulloch, H. J. Egelhaaf, C. J. Brabec, *Energy Environ. Sci.*, 2018, **11**, 2225-2234.
39. K.-M. Huang, C.-M. Lin, S.-H. Chen, C.-S. Li, C.-H. Hu, Y. Zhang, H.-F. Meng, C.-Y. Chang, Y.-C. Chao, H.-

W. Zan, L. Huo, P. Yu, *Sol. RRL*, 2019, **3**, 1900071.

40. S. Dong, T. Jia, K. Zhang, J. Jing, F. Huang, *Joule*, 2020, **4**, 2004-2016.
41. J. H. Jeong, M. Jahandar, A. Prasetio, J. M. Kim, J. H. Kim, S. Kim, D. C. Lim, *Chem. Eng. J.*, 2021, **419**, 129672.
42. X. Huang, D. Fan, S. R. Forrest, *Org. Electron.*, 2021, **97**, 109276.
43. S. Rasool, J. W. Kim, H. W. Cho, Y. J. Kim, D. C. Lee, C. B. Park, W. Lee, O. H. Kwon, S. Cho, J. Y. Kim, *Adv. Energy Mater.*, 2022, **13**, 2203452.
44. Q. Wu, Y. Yu, X. Xia, Y. Gao, T. Wang, R. Sun, J. Guo, S. Wang, G. Xie, X. Lu, E. Zhou, J. Min, *Joule*, 2022, **6**, 2138-2151.
45. C.-S. Tsao, C.-M. Chuang, H.-C. Cha, Y.-Y. Huang, Y.-M. Sung, T.-Y. Chung, Y.-T. Chang, Z.-C. Hu, T.-C. Liu, W.-Y. Ma, Y.-H. Wang, K.-P. Chang, Y.-C. Chao, H.-F. Meng, *Mater. Today Energy,* 2023, **36**, 101340.
46. Y. M. Sung, C. S. Tsao, H. C. Cha, W. Y. Ma, *Prog Photovolt Res Appl.*, 2023, **31**, 803-812.
47. A. Sharma, N. Gasparini, A. Markina, S. Karuthedath, J. Gorenflot, H. Xu, J. Han, A. Balawi, W. Liu, D. Bryant, J. Bertrandie, J. Troughton, S. H. K. Paleti, H. Bristow, F. Laquai, D. Andrienko, D. Baran, *Adv. Mater*., 2024, **36**, 2305367.
48. M. F. Albab, M. Jahandar, Y. H. Kim, Y.-K. Kim, M. Shin, A. Prasetio, S. Kim, D. C. Lim, *Nano Energy,* 2024, **121**, 109219.